RSC Advances

ROYAL SOCIETY OF CHEMISTRY

www.rsc.org/advances

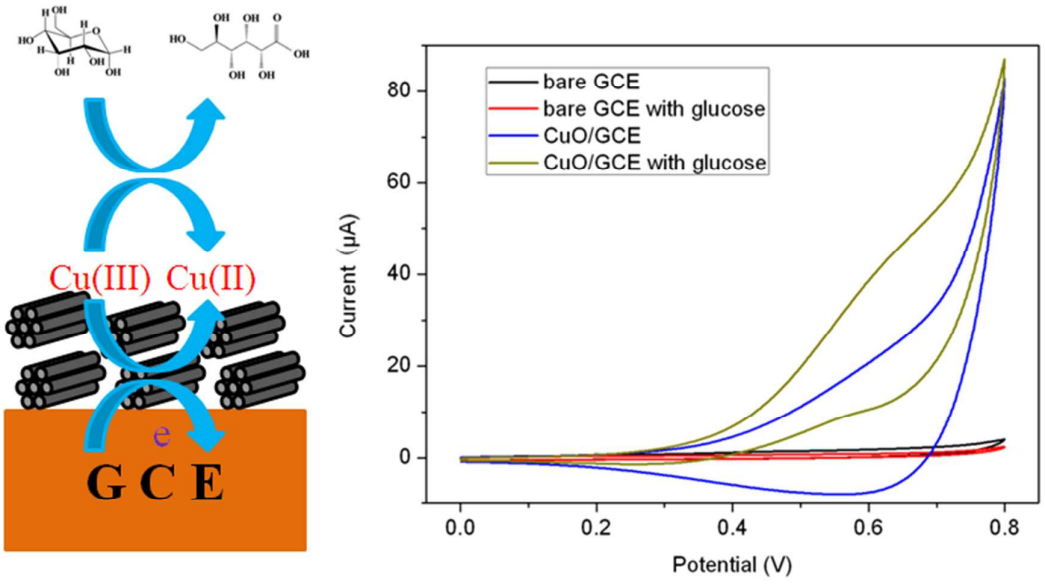

High surface area mesoporous CuO has been successfully used to construct biosensor for enzymatic glucose sensing.

Cite this: DOI: 10.1039/c0xx00000x

www.rsc.org/xxxxxx

ARTICLE TYPE

High surface area mesoporous CuO: A high-performance electrocatalyst for non-enzymatic glucose biosensing

Sen Liu, Ziying Wang, Fengjiao Wang, Bo Yu, and Tong Zhang*

Received (in XXX, XXX) XthXXXXXXXXX 20XX, Accepted Xth XXXXXXXXX 20XX

DOI: 10.1039/b000000x

A highly sensitive and selective non-enzymatic glucose biosensor has been successfully constructed using high surface area mesoporous CuO (108 m^2 g^{-1}) templated by mesoporous carbon. The glucose biosensor exhibits a low detection limit of 0.23 μM at a signal-to-noise ratio of 3.

Introduction

The determination of glucose has received considerable attention due to its wide applications in the fields of medicine, biotechnology, and food industry.[1,2] Among the detection techniques, including electrochemical detection,[3] colorimetric detection,[4] fluorescent detection,[5] as well as Surface-Enhanced Raman Scattering (SERS) method,[6] electrochemical technique is a promising tool for the construction of simple and low-cost glucose biosensors owning to its unique advantages of high sensitivity, good selectivity, and ease of operation.[7,8] It is well known that the conventional glucose biosensors based on glucose oxidase (GOx) exhibit high sensitivity and selectivity for glucose detection. However, these methods exhibit some serious disadvantages, such as complicated and multi-step immobilization procedures, thermal and chemical instability and high cost, limiting their wide applications.[9-11] To overcome these problems, non-enzymatic glucose biosensors based on noble metals (such as, Pt, Pd, Au) have been successfully developed. Unfortunately, the high cost of the electrode materials still limits their commercial applications on a large scale.[12,13]

Recently, much effort has been devoted for developing non-enzymatic glucose biosensors based on low-cost transition metal oxides, such as, CuO, NiO, Co_3O_4, Mn_3O_4 etc.[14-17] Among them, CuO, an important p-type metal oxide semiconductor with narrow band gap (1.2-1.9 eV), has been studied intensely for non-enzymatic glucose biosensing because of its good electrochemical activity, suitable surface charge and easily tunable surface structure. Due to the good stability of CuO materials than that of GO_x, CuO-based non-enzymatic glucose sensors are good candidates for in vitro monitoring of glucose, which is also another reason for development of CuO-based electrochemical glucose biosensors. Up to now, numerous non-enzymatic glucose biosensors based on CuO-based materials have been successfully fabricated. For example, the CuO-based materials with various morphologies or structures, such as nanoparticles,[18] sandwich-structured,[19] nanoflowers,[20] nanofibers,[21] flowers and nanorods,[22] and nanotube arrays[23] have been used for fabrication of non-enzymatic glucose biosensors. Additionally, recent research has shown that sensing performances can be improved by using CuO-based hybrids as sensing materials. Indeed, CuO-carbon nanotubes (CNTs),[24,25] CuO-reduced graphene oxide (rGO),[26] CuO/TiO_2 hierarchical nanocomposites,[27] Pt-doped CuO nanofibers,[28] and CuO-mesoporous carbon[29] have been successfully used for fabrication of non-enzymatic glucose biosensors. However, most of these modified electrodes exhibit more or less drawbacks, such as high cost, the use of complicated instruments for preparation of nanofibers and the rigorous experiment conditions for preparation of CNTs or rGO.

It is well known that surface area of electrocatalysts plays an important role in sensing performances for electrochemical detection and increasing the surface area of electrocatalysts has been proven as an effective stagey for enhancing electrochemical sensing properties.[30,31] Since the first reported in 1992, ordered mesoporous materials have received much attention due to their excellent properties of high surface area, large pore volume as well as uniform mesopores.[32,33] However, there are few reports on development of non-enzymatic glucose biosensors using mesoporous CuO with high surface area as sensing materials.[34]

In this work, a novel non-enzymatic glucose biosensor has been successfully developed using high surface area mesoporous CuO (108 m^2 g^{-1}) as sensing materials. Most importantly, mesoporous CuO exhibits good sensing performances including high sensitivity and high selectivity, which are attributed to its high surface area and open mesopores.

Results and discussion

It is well known that CuO can be dissolved in NaOH solution or HF solution, and thus no mesoporous CuO was obtained by conventional nanocasting method using SBA-15 as hard template. In the present work, mesoporous CuO was prepared using ordered mesoporous carbon CMK-3 as hard template, where three synthesis steps were carried out. Firstly, SBA-15 was prepared using Pluronic P123 ($EO_{20}PO_{70}EO_{20}$, M = 5800) as soft template and tetraethyl orthosilicate (TEOS) as silica source.[35] Fig. S1 shows the small-angle X-ray diffraction (XRD) pattern of SBA-15 after calcination. It is seen that the sample exhibits three well resolved diffraction peaks, which are indexed as (1 0 0), (1 1 0) and (2 0 0) diffractions associated with *p6mm* hexagonal symmetry, indicating the successful preparation of SBA-15.[36]

Secondly, CMK-3 was prepared by using SBA-15 as hard template and sucrose as carbon source.[37] Fig. S2 shows small-angle XRD pattern of CMK-3 after calcination in N_2 at 900 ºC for 4 h, which exhibits a strong diffraction peak, indicating the successful preparation of mesoporous carbon materials.

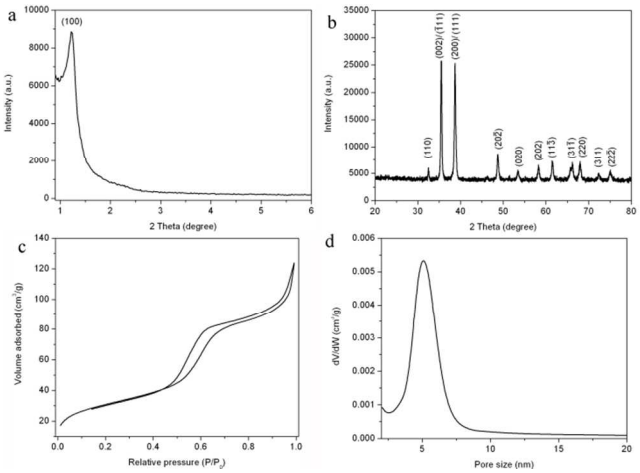

Fig. 1 (a) Small-angle XRD pattern, (b) wide-angle XRD pattern, (c) N_2 adsorption-desorption isothermal and (d) pore size distribution curve of mesoporous CuO thus obtained.

Thirdly, mesoporous CuO was prepared by the nanocasting method using CMK-3 as hard template.[38] Fig. 1a show the small-angle XRD pattern of samples thus obtained, revealing a well resolved diffraction peak at 2θ of 1.23º, which indicates the formation of mesoporous structure. Fig. 1b shows the wide-angle XRD pattern of the mesoporous materials. It is seen that the samples exhibit several diffraction peaks attributed to monoclinic symmetry of CuO (JCPDS Card no. 48-1548).[39] Note that no other peaks attributed to metal Cu, $Cu(OH)_2$ or Cu_2O are observed, indicating the formation of pure phase of CuO.

The formation of mesoporous CuO materials was further confirmed by N_2 isothermal. Fig. 1c shows the N_2 adsorption and desorption isothermal of mesoporous CuO. It is seen that mesoporous CuO exhibits a typical IV-type isotherm with a sharp capillary condensation step at medium relative pressures and a H1 hysteresis loop, suggesting the existence of mesopores, which is in good agreement with ordered mesoporous CuO.[37] Fig. 1d shows pore size distribution curve of mesoporous CuO, indicating that the mesoporous CuO has a uniform pore structure and narrow pore size distribution around 5.1 nm, which also provides another piece of evidence to support the formation of the mesoporous structure. The BET surface area and pore volume of mesoporous CuO are 108 m^2 g^{-1} and 0.16 cm^3 g^{-1}, respectively, further confirming the formation of the mesoporous structure. All these observations indicate that mesoporous CuO has been successfully prepared by nanocasting method using CMK-3 as hard template.

It should be noted that the surface area of mesoporous CuO in this work is higher than that of previously reported CuO materials, such as, hierarchical hollow mesoporous CuO microspheres (51 m^2 g^{-1}),[40] CuO mesoporous nanosheet cluster array (35.82 m^2 g^{-1}),[41] and mesoporous CuO microspheres (65.28 m^2 g^{-1}).[42] The presence of mesoporous structure with high surface area could enhance the interaction between the CuO and glucose molecules, possible improving the sensing performances for glucose detection.

The morphology of the mesoporous CuO was characterized by scanning electron microscopy (SEM). Fig. S3 shows the SEM images of mesoporous CuO, revealing the samples are aggregates with the size about several micrometers, which are consisting of nanorods with the size of 300-500 nm. The corresponding high magnification SEM (Fig. S3b) exhibits these nanorods are also consisting of the nanoparticles below 100 nm.

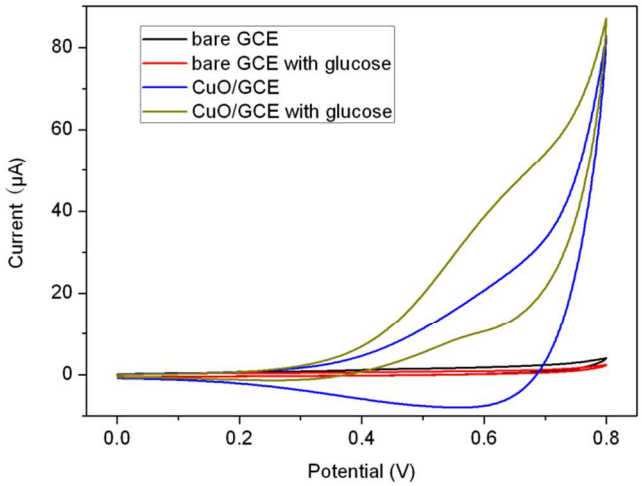

Fig. 2 Cyclic voltammograms (CVs) of bare GCE and CuO/GCE in the absence and in the presence of 2 mM glucose in 0.1 M NaOH (scan rate: 0.05 V s^{-1}).

To demonstrate the electrochemical application of mesoporous CuO, non-enzymatic glucose biosensors were constructed by dropping the aqueous dispersion of mesoporous CuO on the surface of GCE. The sensing performances of both bare GCE and mesoporous CuO modified GCE (designated as CuO/GCE) toward the oxidation of glucose were examined by cyclic voltammetry (CV). Fig. 2 shows the CVs of bare GCE and CuO/GCE in the absence and presence of 2 mM glucose in 0.1 M NaOH. It is seen that bare GCE exhibits no obvious response both in the absence and presence of glucose, indicating that bare GCE exhibits no electrocatalytic activity toward electrochemical oxidation of glucose. In contrast, CuO/GCE exhibits a broad reduction peak at +0.56 V in the alkaline solution, which is attributed to a Cu(II)/Cu(III) redox couple.[43] However, the corresponding oxidation peak of Cu(II)/Cu(III) redox couple is not clearly observed, which may be overlaid by the oxidation peak of water-splitting.[24] Upon addition of 2 mM glucose, CuO/GCE exhibits an obvious oxidation peak attributed to irreversible oxidation of glucose at +0.60 V, indicating that mesoporous CuO can catalyze oxidation of glucose. Fig. 3 shows the schematic of modified electrode structure and the reaction pathway during the non-enzymatic electrochemical oxidation of glucose on the surface of the CuO/GCE in an alkaline medium. All these observations indicate that mesoporous CuO exhibits electrocatalytic ability toward oxidation of glucose and can be used for fabrication of non-enzymatic glucose biosensor.

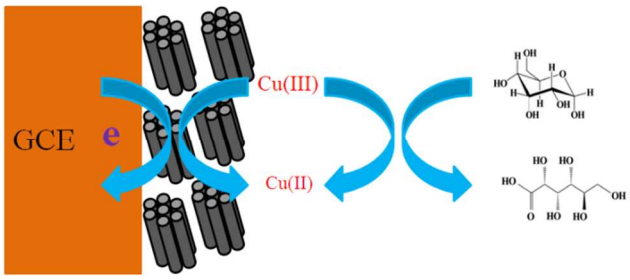

Fig. 3 Schematic of modified electrode structure and the reaction pathway during the non-enzymatic electrochemical oxidation of glucose on the surface of the CuO/GCE in 0.1 M NaOH.

Fig. 4 shows the typical amperometric response curve of CuO/GCE in 0.1 M NaOH solution on successive step-wise change of glucose concentrations at the applied potential of +0.6 V. The inset of Fig. 4 shows the response curve of CuO/GCE toward low concentrations of glucose ranging from 0.5 μM to 100 μM. Additionally, the amperometric response curves of CuO/GCE to various concentrations of glucose were also examined with applied potential of +0.5 V and +0.7 V, respectively, as shown in Fig. S4a and Fig. S4b. It should be noted that an obvious response was observed at CuO/GCE by addition of 0.5 μM glucose, indicating the high sensitivity of this glucose biosensor. When an aliquot of glucose was added into the NaOH solution with stirring, CuO/GCE responded rapidly to the substrate and the current rose steeply to reach a stable value. The anode current of the sensor increased dramatically and achieved 95% of the steady state current within 2 s, revealing a fast amperometric response behavior. In contrast, the sensors exhibit no obvious response to low concentration of glucose with the applied potential of +0.5 V and +0.7 V. Thus, the optimized applied potential for amperometric response curve is +0.6 V.

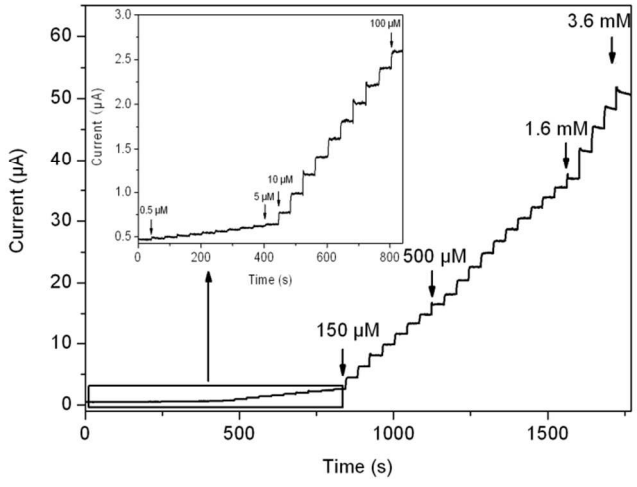

Fig. 4 Typical steady-state response of the CuO/GCE to successive injection of glucose into the 0.1 M NaOH solution under stirring. The inset was the response of the CuO/GCE toward the concentration of glucose ranging from 0.5 μM to 100 μM (applied potential: +0.6 V).

Fig. 5 shows the calibration curve of the sensor for increasing the concentrations of glucose from 0.5 μM to 3.6 mM. The intensity of response toward the oxidation of glucose increased with increasing the concentrations of glucose, indicating that the glucose biosensor thus constructed can be used for detection of glucose at a wide concentration range. The insets in Fig. 5 show the calibration curves for the low concentrations of glucose, revealing that the biosensor exhibits good linear detection ranging from 0.5 μM to 5 μM (r = 0.998) and 10 μM to 100 μM (r = 0.999), respectively. The detection limit is estimated to be 0.23 μM at a signal-to-noise ratio of 3. It should be noted that our present sensing system gives a lower detection limit than those of the biosensors for detection of glucose, such as CuO nanoparticles (0.5 μM),[18] sandwich-structured CuO (1.0 μM),[19] CuO nanofibers (0.8 μM),[21] CuO flowers and nanorods (4 μM),[22] and CuO loaded SBA-15 (10 μM).[44] The performance of our glucose sensor is also compared with those previously published non-enzymatic glucose sensors based on CuO materials, as shown in Table 1.

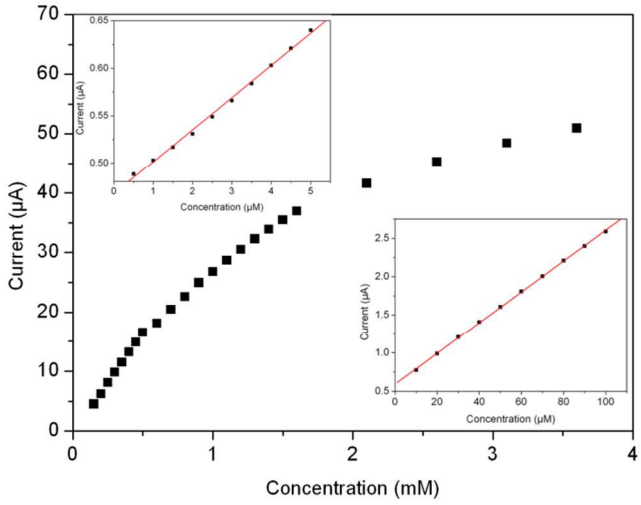

Fig. 5 The calibration curve for the amperometric response of the CuO/GCE. The insets were the calibration curve with the glucose concentration increasing from 0.5 μM to 5 μM and 10 μM to 100 μM, respectively (applied potential: +0.6 V).

It is well know that ascorbic acid (AA) and uric acid (UA) are the most important interferences normally co-existing with glucose in blood plasma. In the physiological sample, glucose concentration (4-7 mM) is generally much higher than those of interfering species.[45] Thus, interference tests were carried out by adding 1.0 mM glucose in 0.1 M NaOH solution, followed with additions of 0.1 mM AA, 0.1 mM UA and other possible interference such as ethanol (10 mM). Fig. 6 shows the corresponding response curve. It is seen that a strong oxidation current is obtained by addition of 1.0 mM glucose, and no obvious oxidation current is observed after addition of other interferences, such as AA, UA and ethanol, indicating that the glucose biosensor thus obtained based on mesoporous CuO exhibits high selectivity toward electrochemical detection of glucose.[46] The relative standard deviation (RSD) of the amperometric response to 0.1 mM of glucose at +0.6 V is 5.2% for 5 successive measurements, indicating the good reproducibility of CuO/GCE. Furthermore, the variation of the amperometric response current at the CuO/GCE decreases to about 94 % of its initial response current on the 5th day,

indicating the good stability of the glucose sensors thus obtained.

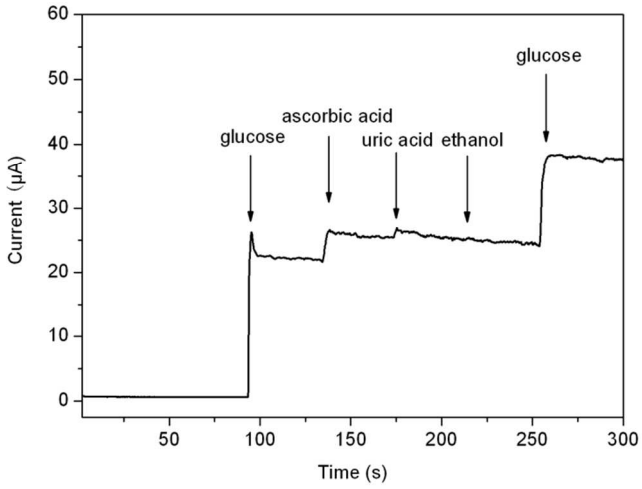

Fig. 6 Interference test of CuO/GCE at +0.6 V in 0.1 M NaOH with 1 mM glucose in the presence of 0.1 mM AA, 0.1 mM UA, and 10 mM ethanol.

Table 1 Comparison of analytical performance of our proposed glucose sensor with other published non-enzymatic glucose sensors based on CuO materials.

Materials	Performances		Refs
	LOD	Linear range	
CuO nanoparticles	0.5μM	5 μM -2.3 mM	[18]
Sandwich-structured CuO	1.0 μM	20 μM -3.2 mM	[19]
CuO nanofibers	0.8 μM	6 μM -2.5 mM	[21]
CuO flowers and nanorods	4 μM	4 μM -8 mM	[22]
CuO-loaded SBA-15	10 μM	50 μM -20 mM	[44]
Mesoporous CuO	0.23 μM	0.5 μM -5 μM; 10 μM -100 μM	This work

Conclusion

A novel non-enzymatic glucose biosensor has been successfully fabricated using mesoporous CuO as sensing materials, which were prepared by the nanocasting method using CMK-3 as template. Our present study is important because it provides a novel method for non-enzymatic detection of glucose by using mesoporous metal oxides as sensing materials, which also suggests the potential applications of the mesoporous CuO for constructing efficient biosensing.

Acknowledgements

This research work was financially supported by the National Natural Science Foundation of China (Grant No. 51202085).

Notes and references

State Key Laboratory on Integrated Optoelectronics, College of Electronic Science and Engineering, Jilin University, Changchun 130012, P. R. China. Fax: +86 431 85168270; Tel: +86 431 85168385; E-mail: zhangtong@jlu.edu.cn

1 C. Zhu, S. Guo and S. Dong, *Adv. Mater.*, 2012, **24**, 2326-2331.
2 C. Wei, X. Li, F. Xu, H. Tan, Z. Li, L. Sun and Y. Song, *Anal. Methods*, 2014, **6**, 1550-1557.
3 S. Park, H. Boo and T. D. Chung, *Anal. Chim. Acta*, 2006, **556**, 46-75.
4 Y. Song, K. Qu, C. Zhao, J. Ren and X. Qu, *Adv. Mater.*, 2010, **22**, 2206-2210.
5 Y. Liu, C. Deng, L. Tang, A. Qin, R. Hu, J. Z. Sun and B. Z. Tang, *J. Am. Chem. Soc.*, **2011**, *133*, 660-663.
6 K. E. Shafer-Peltier, C. L. Haynes, M. R. Glucksberg and R. P. Van Duyne, *J. Am. Chem. Soc.*, 2003, **125**, 588-593.
7 H. Huo, C. Guo, G. Li, X. Han and C. Xu, *RSC Adv.*, 2014, **4**, 20459-20465.
8 S. Liu, B. Yu and T. Zhang, *Electrochim. Acta*, 2013, **102**, 104-107.
9 J. Wang, *Chem. Rev.*, 2008, **108**, 814-825.
10 P. Si, P. Chen and D.-H. Kim, *J. Phys. Chem. B*, 2013, **1**, 2696-2700.
11 S. Liu, J. Tian, L. Wang, Y. Luo, W. Lu and X. Sun, *Biosens. Bioelectron.*, 2011, **26**, 4491-4496.
12 S. Guo, D. Wen, Y. Zhai, S. Dong and E. Wang, *ACS Nano*, 2010, **4**, 3959-3968.
13 Y. Li, Y. Song, C. Yang and X.-H. Xia, *Electrochem. Commun.*, 2007, **9**, 981-988.
14 K. E. Toghill and R. G. Compton, *Int. J. Electrochem. Sci.*, 2010, **5**, 1246-1301.
15 L. Xu, Q. Yang, X. Liu, J. Liu and X. Sun, *RSC Adv.*, 2014, **4**, 1449-1455.
16 Y. Ding, Y. Wang, L. Su, M. Bellagamba, H. Zhang and Y. Lei, *Biosens. Bioelectron.*, 2010, **26**, 542-548.
17 P. Si, X.-C. Dong, P. Chen, and D.-H. Kim, *J. Phys. Chem. B*, 2013, **1**, 110-115.
18 S. Liu, J. Tian, L. Wang, X. Qin, Y. Zhang, Y. Luo, A. M. Asiri, A. O. Al-Youbi and X. Sun, *Catal. Sci. Technol.*, 2012, **2**, 813-817.
19 S. K. Meher and G. R. Rao, *Nanoscale*, 2013, **5**, 2089-2099.
20 S. Sun, X. Zhang, Y. Sun, S. Yang, X. Song and Z. Yang, *Phys. Chem. Chem. Phys.*, 2013, **15**, 10901-10913.
21 W. Wang, L. Zhang, S. Tong, X. Li and W. Song, *Biosens. Bioelectron.*, 2009, **25**, 708-714.
22 X. Wang, C. Hu, H. Liu, G. Du, X. He and Y. Xi, *Sens. Actuators B: Chem.*, 2010, **144**, 220-225.
23 L. Zhang, H. Li, Y. Ni, J. Li, K. Liao and G. Zhao, *Electrochem. Commun.*, 2009, **11**, 812-815.
24 F. Jiang, S. Wang, J. Lin, H. Jin, L. Zhang, S. Huang and J. Wang, *Electrochem. Commun.*, 2011, **13**, 363-365.
25 L.-C. Jiang and W.-D. Zhang, *Biosens. Bioelectron.*, 2010, **25**, 1402-1407.
26 Y.-W. Hsu, T.-K. Hsu, C.-L. Sun, Y.-T. Nien, N.-W. Pu and M.-D. Ger, *Electrochim. Acta*, 2012, **82**, 152-157.
27 J. Chen, L. Xu, R. Xing, J. Song, H. Song, D. Liu and J. Zhou, *Electrochem. Commun.*, 2012, **20**, 75-78.
28 W. Wang, Z. Li, W. Zheng, J. Yang, H. Zhang and C. Wang, *Electrochem. Commun.*, 2009, **11**, 1811-1814.
29 H. Wu, S. Zhou, Y. Wu and W. Song, *J. Mater. Chem. A*, 2013, **1**, 14198-14205.
30 J. C. Ndamanisha and L. Guo, *Biosens. Bioelectron.*, 2008, **23**, 1680-1685.
31 J. C. Ndamanisha and L. Guo, *Anal. Chim. Acta*, 2012, **747**, 19-28.
32 C. T. Kresge, M. E. Leonowicz, W. J. Roth, J. C. Vartuli and J. S. Beck, *Nature*, 1992, **359**, 710-712.
33 S. Liu, H. Li, L. Wang, J. Tian and X. Sun, *J. Mater. Chem.*, 2011, **21**, 339-341.
34 M.-F. Wang, Q.-A. Huang, X.-Z. Li and Y. Wei, *Anal. Methods*, 2012, **4**, 3174-3179.
35 S. Liu, H. Zhang, X. Meng, Y. Zhang, L. Ren, F. Nawaz, J. Liu, Z. Li and F.-S. Xiao, *Micropor. Mesopor. Mater.*, 2010, **136**, 126-131.
36 D. Zhao, J. Feng, Q. Huo, N. Melosh, G. H. Fredrickson, B. F. Chmelka and G. D. Stucky, *Science*, 1998, **279**, 548-552.
37 L. Wang, S. Lin, K. Lin, C. Yin, D. Liang, Y. Di, P. Fan, D. Jiang and F.-S. Xiao, *Micropor. Mesopor. Mater.*, 2005, **85**, 136-142.
38 X. Lai, X. Li, W. Geng, J. Tu, J. Li and S. Qiu, *Angew. Chem. Int. Ed.*, 2007, **46**, 738-741.
39 B. Zhao, P. Liu, H. Zhuang, Z. Jiao, T. Fang, W. Xu, B. Lu and Y. Jiang, *J. Mater. Chem. A*, 2013, **1**, 367-373.

40 S. Ghosh and M. K. Naskar, *RSC Adv.*, 2013, *3*, 13728-13733.
41 X. Chen, N. Zhang and K. Sun, *J. Mater. Chem.*, 2012, **22**, 13637-13642.
42 Z. Zhang, H. Chen, X. She, J. Sun, J. Teo and F. Su, *J. Power Sources*, 2012, **217**, 336-344.
43 N. Q. Dung, D. Patil, H. Jung and D. Kim, *Biosens. Bioelectron.*, 2013, **42**, 280-286.
44 M. U. Anu Prathap, B. Kaur and R. Srivastava, *J. Colloid Interf. Sci.*, 2012, **381**, 143-151.
45 S.-J. Li, N. Xia, X.-L. Lv, M.-M. Zhao, B.-Q. Yuan and H. Pang, *Sens. Actuators B*: *Chem.*, 2014, **190**, 809-817.
46 X.-Y. Lang, H.-Y. Fu, C. Hou, G.-F. Han, P. Yang, Y.-B. Liu and Q. Jiang, *Nat. Commun.*, 2013, **4**, 2169.